ELSEVIER

International Journal of Pressure Vessels and Piping 78 (2001) 261–269

INTERNATIONAL JOURNAL OF
Pressure Vessels and Piping

www.elsevier.com/locate/ijpvp

Probabilistic fracture mechanics for nonlinear structures

S. Rahman[1,*], J.S. Kim

Department of Mechanical Engineering, The University of Iowa, 2140 Seamans Center, Iowa City, IA 52242, USA

Received 28 June 2000; revised 23 December 2000; accepted 6 January 2001

Abstract

A probabilistic methodology has been developed for fracture-mechanics analysis of nonlinear cracked structures. The methodology involves nonlinear finite element analysis using well-known commercial codes; statistical models for uncertainty in material constitutive law, fracture toughness, and loads; and standard reliability methods for evaluating probabilistic characteristics of elastic–plastic fracture parameter. Numerical examples are presented to illustrate the proposed methodology for two- and three-dimensional cracked structures. The results from these examples show that the methodology is capable of predicting accurate deterministic and probabilistic characteristics of the *J*-integral for use in elastic–plastic fracture mechanics (EPFM).

Keywords: Probabilistic fracture mechanics; Elastic–plastic fracture mechanics; *J*-integral; Crack; First-order reliability method; Second-order reliability method; Monte Carlo with importance sampling

1. Introduction

Probabilistic fracture mechanics (PFM) is a rapidly developing field, with numerous applications in science and engineering. The fundamental theory of fracture mechanics establishes a mechanistic relationship between the maximum permissible loads acting on a structural component to the size and location of a crack — either real or postulated — in the component. Fracture analysis can be based on linear-elastic or more complex elastic–plastic (nonlinear) models. It is well established that nonlinear fracture-mechanics methods, compared with the elastic methods [1,2], provide more realistic measures of fracture behavior of cracked structures with high toughness and low strength materials. Cracked components composed of these materials, when used in nuclear power plants, chemical and fossil plants, automobiles, and aerospace and aircraft propulsion systems, pose a serious threat to structural integrity. In much or all of the working temperature regime of these components, the material is typically stressed above the brittle-to-ductile transition temperature where the fracture response is essentially ductile, and the material is capable of considerable inelastic deformation [1,2]. As such, elastic–plastic theories should be employed in fracture analyses of these structural components. While development is still ongoing, significant progress has been made in deterministic modeling of linear-elastic fracture mechanics (LEFM) and elastic–plastic fracture mechanics (EPFM). Probabilistic models have also been developed to estimate various response statistics and reliability [3]. Currently, there are many methods and applications for PFM in the oil and gas, nuclear, automotive, naval, aerospace, and other industries, nearly all of which have been developed based on LEFM models. In contrast, probabilistic analyses based on EPFM models are not widespread and are only currently gaining notice, particularly for applications in pressure boundary components.

In EPFM, the crack-driving force is frequently described in terms of the *J*-integral. The *J*-integral is an appropriate fracture parameter to adequately describe crack-tip stress and strain fields when there are no constraint effects. Similar to any deterministic EPFM problem, the evaluation of the *J*-integral for probabilistic analysis can be performed by either a numerical method and or an engineering estimation method. Traditionally, the numerical study is based on the elastic–plastic finite element method (FEM). Using FEM, one can calculate *J* for any crack geometry and load conditions. However, it is also useful to employ simplified estimation methods for routine engineering calculations. Accordingly, probabilistic EPFM analyses based on both methods have been reported. For example, in the U.S. Nuclear Regulatory Commission's *Short Cracks in Piping and Piping Welds Program* [4], a probabilistic model was developed by the first author for elastic–plastic analysis of

* Corresponding author. Tel.: +1-319-335-5679; fax: +1-319-335-5669.
E-mail address: rahman@engineering.uiowa.edu (S. Rahman).
[1] Website: http://www.engineering.uiowa.edu/~rahman

0308-0161/01/$ - see front matter
PII: S0308-0161(01)00006-0

circumferential through-wall cracks in pipes for leak-before-break applications [5]. This model involves a J-estimation method, statistical representation of uncertainties in loads, crack size, and material properties, and first- and second-order reliability methods (FORM/SORM). Shortly thereafter, similar probabilistic models based on other J-estimation formulas were reported [6–9]. In these models, estimation formulas typically consist of a closed-form response surface approximation of J as a function of load, crack size, and material properties of the structure and hence, do not require costly finite element calculations. Essentially, this presents a primary rationale for successful development of FORM/SORM algorithms for probabilistic analysis of elastic–plastic structures [5–9]. However, the usefulness of J-estimation based methods is limited, since they cannot be applied to general fracture-mechanics analysis. Because of the complexity in crack geometry, external loads, and material behavior, more advanced computational tools, such as FEM or other numerical methods, must be employed to provide the necessary computational framework for analysis of general cracked structures. Furthermore, due to various approximations in the J-estimation method, one needs to evaluate its accuracy by comparing with generally more accurate FEM-based probabilistic analysis [10]. To date, not many PFM analyses involving nonlinear FEM have been conducted or reported.

This paper presents a computational methodology for stochastic prediction of elastic–plastic fracture parameters and probabilistic characterization of fracture initiation in nonlinear cracked structures. The methodology is based on (1) nonlinear finite element method for deterministic stress analysis, (2) statistical models for loads and material properties, including stress–strain and fracture toughness curves, and (3) standard computational methods of structural reliability theory for probabilistic analysis. The computer code PRObabilistic FRActure Code (PROFRAC) was developed by implementing all the numerical methods employed in this study. Two examples are presented to illustrate the proposed methodology for two- and three-dimensional cracked structures. The results from these examples show that the methodology is capable of predicting accurate deterministic and probabilistic characteristics of the J-integral for use in EPFM.

2. Elastic–plastic fracture mechanics

In order to perform elastic–plastic analysis, the material model must be defined. This study assumed that the constitutive law characterizing the material's stress–strain (σ–ϵ) response could be represented by the well-known Ramberg–Osgood model, expressed as

$$\frac{\epsilon}{\epsilon_0} = \frac{\sigma}{\sigma_0} + \alpha\left(\frac{\sigma}{\sigma_0}\right)^n, \tag{1}$$

where σ_0 is the reference stress (typically assumed to be the yield stress), E the modulus of elasticity, $\epsilon_0 = \sigma_0/E$ the associated reference strain, and α and n are model parameters usually selected from a best fit of actual laboratory data. Although this representation of the stress–strain curve is not necessary for finite element analysis, it is required for most, if not all, J-estimation methods.

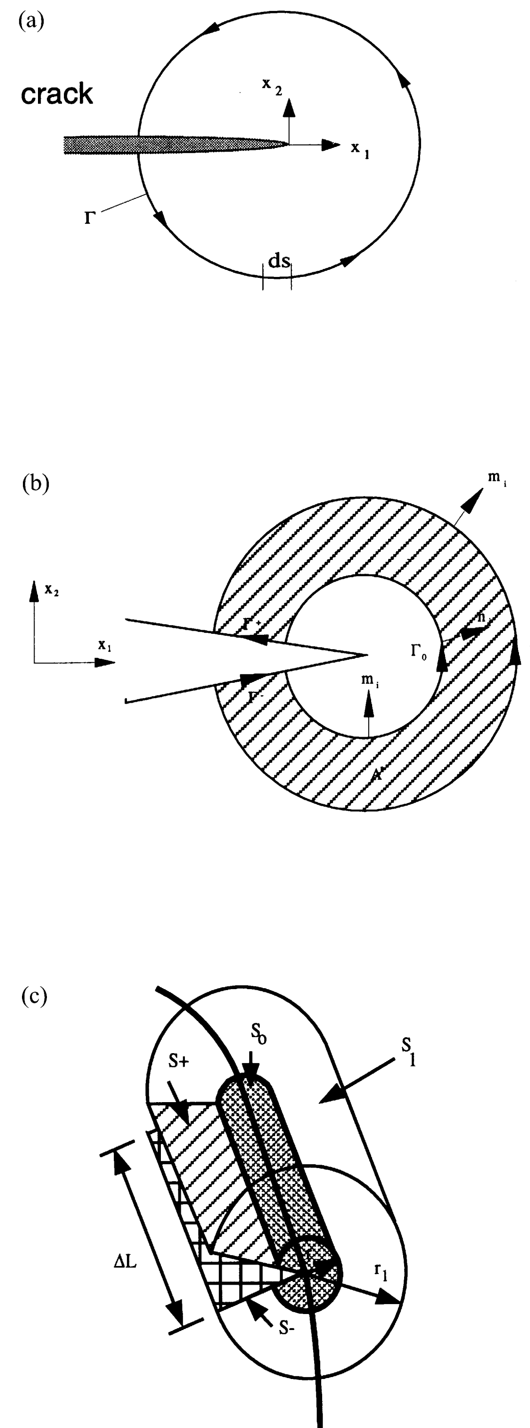

Fig. 1. J-integral as an elastic–plastic fracture parameter: (a) arbitrary contour around a crack tip; (b) inner and outer contours enclosing A^*; (c) inner and outer surfaces enclosing V^*.

The J-integral parameter proposed by Rice [11] has been extensively used in assessing the fracture integrity of cracked engineering structures, which undergo large plastic deformation at the crack tip. For elastic–plastic problems, the Hutchinson [12] and Rice and Rosengren [13] interpretation of the J-integral parameter as the strength of the asymptotic crack-tip fields represents the crux of the basis for *J-controlled* crack growth behavior. For a cracked body with an arbitrary counter-clockwise path Γ around the crack tip (see Fig. 1(a)), a formal definition of J under the mode-I condition is

$$J \overset{\text{def}}{=} \int_{\Gamma} (\omega n_1 - T_i u_{i,1})\, \mathrm{d}s, \tag{2}$$

where, $\omega = \int \sigma_{ij}\, \mathrm{d}\epsilon_{ij}$ is the strain energy density with σ_{ij} and ϵ_{ij} representing of components of stress and strain tensors, respectively, u_i and $T_i = \sigma_{ij} n_j$ are the ith components of displacement and traction vectors, n_j is the jth component of the unit outward normal to the integration path, ds is the differential length along contour Γ, and $u_{i,1} = \partial u_i / \partial x_1$ is the differentiation of displacement with respect to x_1. The summation convention is adopted here for repeated indices.

The J-integral is theoretically valid for nonlinear elasticity or deformation theory of plasticity where little or no unloading occurs. The J-integral is frequently used to characterize initiation of crack growth and a small amount of crack propagation. Numerous comparisons between predictions based on J-integral and experimental data have shown that fairly accurate results of fracture response can be obtained for monotonic loading to failure, even though the theoretical conditions for a valid J-based fracture theory are violated [14–17]. In this study, the elastic–plastic analysis of cracks will focus only on the J-integral fracture parameter.

2.1. Finite element implementation of J-integral

The energy domain integral methodology [18,19] was used in the finite element analysis to numerically calculate J. Using the divergence theorem, the contour integral defined in Eq. (1) can be expanded into an area integral in two dimensions and a volume integral in three dimensions over a finite domain surrounding the crack tip or crack front. For two- dimensional quasi-static problems involving linear or nonlinear elastic materials and no body forces, thermal strains, and crack-face tractions, Eq. (1) reduces to

$$J = \int_{A^*} \left[\sigma_{ij} \frac{\partial u_j}{\partial x_1} - w\delta_{1i} \right] \frac{\partial q}{\partial x_i}\, \mathrm{d}A, \tag{3}$$

where δ_{ij} is Kronecker delta, q an arbitrary, but smooth, weighting function equal to *unity* on Γ_0 and *zero* on Γ_1, and A^* is the annular area enclosed by the inner contour Γ_0 and outer contour Γ_1 as shown in Fig. 1(b). For three-dimensional problems, a similar expression of J that involves the volume integral can be developed and is given by

$$J = \int_{V^*} \left[\sigma_{ij} \frac{\partial u_j}{\partial x_1} - w\delta_{1i} \right] \frac{\partial q}{\partial x_i}\, \mathrm{d}V, \tag{4}$$

where V^* is the volume enclosed by the inner surface S_0 and outer surface S_1, as shown in Fig. 1(c). The discrete form of these domain integrals is [20]

$$J \cong \sum_{A^* \text{ or } V^*} \sum_{l=1}^{m} \left\{ \left[\left(\sigma_{ij} \frac{\partial u_j}{\partial x_1} - w\delta_{1i} \right) \frac{\partial q}{\partial x_i} \right] \left| \frac{\partial x_j}{\partial \xi_k} \right| \right\}_l w_l, \tag{5}$$

where m is the number of Gauss points per element, ξ_k the parametric coordinate, and w_l is the weighting factor. Further details on finite element implementation of J can be found in Anderson [20].

2.2. J-based failure criteria

Given that J is a valid fracture parameter, there are several definitions of failure criteria. Two definitions, commonly used in EPFM, are (1) initiation of crack growth and (2) unstable crack growth [14–17], described by

$$\text{Crack initiation}: \; J = J_{Ic}, \tag{6}$$

$$\text{Crack instability}: \begin{cases} J = J_R \\ \dfrac{\partial J}{\partial a} = \dfrac{\mathrm{d}J_R}{\mathrm{d}a} \end{cases}. \tag{7}$$

The initiation of crack growth in a structure containing flaws can be characterized by the crack-driving force (J) exceeding the material fracture toughness (J_{Ic}), as represented in Eq. (6). This constitutes a good definition of failure, when the uncracked ligament is small (e.g. part-through surface cracks in pipes or through-wall cracks in small-diameter pipes) or the amount of subsequent stable crack growth is limited (e.g. cracks in brittle materials). The initiation-based failure criterion is commonly used in piping and pressure vessel analysis [14–17].

In elastic–plastic fracture-mechanics theory, stable crack growth, when occurring in a structure, can also be characterized by the J-integral parameter with some limitations. In this regard, the J-tearing theory is a prominent concept to quantify stable crack growth. The J-tearing theory is based on the observation that fracture instability can occur subsequent to some amount of stable crack growth in tough and ductile materials with an attendant higher applied load level at fracture. The onset of fracture instability is defined when J and $\partial J/\partial a$ exceed J_R and $\mathrm{d}J_R/\mathrm{d}a$ simultaneously, as also expressed in Eq. (7). The corresponding crack-instability load is either equal to or higher than the crack-initiation load. The difference between these two failure loads can be significant if the structural geometry and material permit an appreciable amount of stable crack growth. Otherwise, the fracture criterion based on the initiation of crack growth provides a conservative estimate of structural integrity. This initiation-based criterion was used in the probabilistic fracture analysis to be presented in forthcoming sections.

3. Random parameters and fracture response

Consider a cracked structure with uncertain mechanical and geometric characteristics that is subject to random loads. Denote by $\mathbf{X}$ an N-dimensional random vector with components $X_1, X_2, \ldots, X_N$ characterizing all uncertainty in the system and load parameters. Let J be a relevant crack-driving force that can be calculated using elastic–plastic finite element analysis. If J is a valid fracture parameter, it can be applied to determine the failure probability of the cracked structure. Suppose the structure fails when $J > J_{Ic}$. This requirement cannot be satisfied with certainty, because J depends on input vector $\mathbf{X}$ which is random and J_{Ic}, itself is a random variable. Hence, the performance of the cracked structure should be evaluated by the reliability P_S or its complement, the probability of failure $P_F (P_s = 1 - P_F)$, defined as

$$P_F \stackrel{\text{def}}{=} \Pr[g(X) < 0] \stackrel{\text{def}}{=} \int_{g(\mathbf{x})<0} f_X(\mathbf{x})\,d\mathbf{x}, \tag{8}$$

where $f_{\mathbf{X}}(\mathbf{x})$ is the joint probability density function of $\mathbf{X}$, and $g(\mathbf{X})$ is the performance function given by

$$g(\mathbf{X}) = J_{Ic}(\mathbf{X}) - J(\mathbf{X}). \tag{9}$$

Note that P_F in Eq. (8) represents the probability of the initiation of crack growth, which provides a conservative estimate of structural performance. A less conservative evaluation requires calculation of the failure probability based on crack-instability criterion. The latter probability is more difficult to compute since it must be obtained by incorporating crack-growth simulation in a nonlinear finite element analysis. However, if suitable approximations of J can be developed analytically, the crack-instability failure probability can be easily calculated, as demonstrated by previous research in probabilistic pipe fracture evaluations [5,6].

4. Structural reliability analysis

The generic expression for the failure probability in Eq. (8) involves a multidimensional probability integration for its evaluation. In this study, standard reliability methods, such as FORM/SORM [21], and Monte Carlo with importance sampling (MCIS) [22]were used to compute these probabilities. These standard reliability methods are briefly described here to compute the probability of failure P_F in Eq. (8) assuming a generic N-dimensional random vector $\mathbf{X}$ and the performance function $g(\mathbf{X})$ from Eq. (9).

4.1. First- and second-order reliability methods

The FORM/SORM are based on linear (first-order) and quadratic (second-order) approximations, respectively, of the limit state surface $g(\mathbf{x}) = 0$ tangent to the closest point of the surface to the origin of the space. The determination of this point involves nonlinear constrained optimization typically performed in the standard Gaussian image of the original space. The FORM/SORM algorithms involve several steps. First, the space of uncertain parameters $\mathbf{x}$ is transformed into a new N-dimensional space $\mathbf{u}$ consisting of independent standard Gaussian variables. The original limit state $g(\mathbf{x}) = 0$ is then mapped into the new limit state $g_U(\mathbf{u}) = 0$ in the $\mathbf{u}$ space. Second, the point on the limit state $g_U(\mathbf{u}) = 0$ having the shortest distance to the origin of the $\mathbf{u}$ space is determined using an appropriate nonlinear optimization algorithm. This point is referred to as the design point or beta point, and has a distance β_{HL}, known as reliability index, to the origin of the $\mathbf{u}$ space. Third, the limit state $g_U(\mathbf{u}) = 0$ is approximated by a surface, tangent to the limit state at the design point. Let such limit states be $g_L(\mathbf{u}) = 0$ and $g_Q(\mathbf{u}) = 0$, which correspond to approximating surfaces as hyperplane (linear or first-order) and hyperparaboloid (quadratic or second-order), respectively. The probability of failure P_F (Eq. (10)) is thus approximated by $\Pr[g_L(\mathbf{u}) < 0]$ in FORM and $\Pr[g_Q(\mathbf{u}) < 0]$ in SORM. These first-order ($P_{F,1}$) and second-order ($P_{F,2}$) estimates are given by [21,22]

$$P_{F,1} = \Phi(-\beta_{HL}),$$

$$P_{F,2} \cong \Phi(-\beta_{HL}) \prod_{i=1}^{N-1} \left(1 - \kappa_i \frac{\phi(-\beta_{HL})}{\Phi(-\beta_{HL})}\right)^{-1/2}, \tag{10}$$

where $\Phi(\cdot)$ is the cumulative distribution function of a

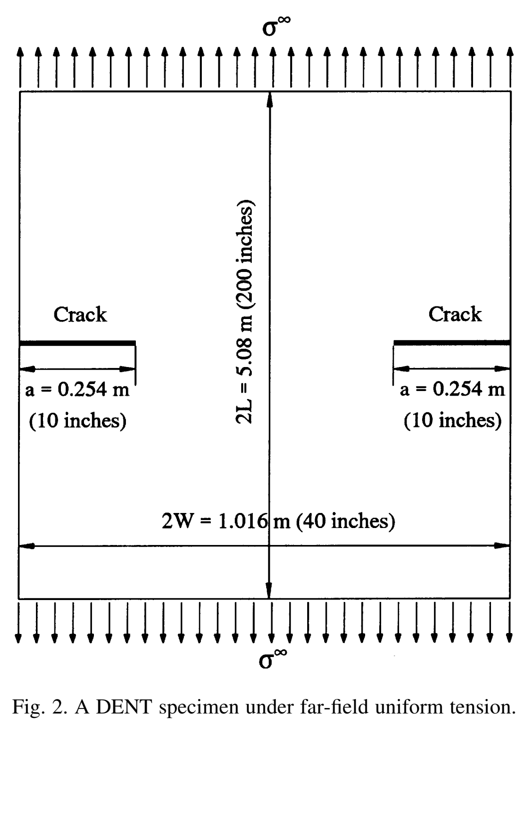

Fig. 2. A DENT specimen under far-field uniform tension.

Table 1
Statistical properties of random input for DENT specimen

Random variable	Mean	COV[a]	Probability distribution	References
Elastic modulus (E)	206.8 GPa	0.05	Gaussian	–[b]
Ramberg–Osgood coefficient (α)	8.073	0.439	Lognormal	5
Ramberg–Osgood exponent (n)	3.8	0.146	Lognormal	5
Initiation fracture toughness (J_{Ic})	1,242.6 kJ/m^2	0.47	Lognormal	5
Far-field tensile stress (σ^∞)	Variable[c]	0.1	Gaussian	–[b]

[a] COV = standard deviation/mean.
[b] Arbitrarily assumed.
[c] Varies from 48.3 to 103.4 MPa (7000–15,000 psi).

standard Gaussian random variable and κ_i's are the principal curvatures of the limit state surface at the design point.

4.2. Monte Carlo with importance sampling

In MCIS, the random variables are sampled from a different probability density referred to as the sampling density. The objective of the importance sampling is to generate more outcomes from the region of interest, e.g. the failure set $\mathscr{F} = \{\boldsymbol{x} : g(\boldsymbol{x}) < 0\}$. Good sampling densities can be constructed using information from FORM/SORM analyses. According to Hohenbichler [22], the failure probability estimate $P_{\mathrm{F,IS}}$ using importance sampling based on SORM improvement is given by

$$P_{\mathrm{F,IS}} \cong \Phi(-\beta_{\mathrm{HL}}) \prod_{i=1}^{N-1} [1 - \kappa_i \Psi(-\beta_{\mathrm{HL}})]^{1/2} \frac{1}{N_{\mathrm{IS}}} \times \sum_{i=1}^{N-1} \frac{\Phi[h_{\mathrm{Q}}(\mathbf{w}_j)]}{\Phi(-\beta_{\mathrm{HL}})} \exp\left[-\frac{1}{2} \Psi(\beta_{\mathrm{HL}}) \sum_{k=1}^{N-1} \kappa_k w_{k,j}^2 \right], \quad (11)$$

where

$$\Psi(-\beta_{\mathrm{HL}}) = \frac{\phi(-\beta_{\mathrm{HL}})}{\Phi(-\beta_{\mathrm{HL}})}, \quad (12)$$

with $\phi(\cdot)$ and $\Phi(\cdot)$ representing the probability density and cumulative distribution functions, respectively, of a standard normal variable, $\mathbf{w}_j = \{w_{1,j}, w_{2j},\ldots, w_{N-1j}\}^{\mathrm{T}}$ is the jth realization of an N − 1 dimensional independent Gaussian random vector $\mathbf{W}$ with the mean and variance of its ith component being *zero* and $1/[1 - \Psi(-\beta_{\mathrm{HL}})]$, respectively, $h_{\mathrm{Q}}(\mathbf{w}_{\mathrm{j}})$ is the quadratic approximant in the form of rotational hyperparaboloid, and N_{IS} is the sample size for importance sampling. Further details are available elsewhere [22].

5. Development of PROFRAC code

The PROFRAC computer code was developed to calculate the probability of failure as defined by Eq. (8). PROFRAC provides a general framework for performing PFM analysis based on J-integral evaluations of two- and three-dimensional cracked structures subject to quasi-static loads. The PROFRAC code is based on (1) state-of-the-art methods of EPFM theory and nonlinear finite element analysis, (2) statistical models of uncertainty for random loads and material properties, and (3) standard computational methods of structural reliability theory. PROFRAC has been enhanced to interface with several commercial codes, including the ABAQUS finite element code [23] and STRUREL probabilistic analysis code [24]. The methods coded in PROFRAC for calculating J and performing subsequent reliability analysis has been described previously herein. Using PROFRAC, the relevant parameters in the input deck of ABAQUS can be modeled as random variables. Both LEFM- and EPFM-based fracture theories are supported. A number of finite element types can be chosen for probabilistic finite element analysis. The probabilistic analysis is completely automated.

A major limitation of the current version of PROFRAC is that it can only calculate probability of failure based on initiation of crack growth. The calculation of failure

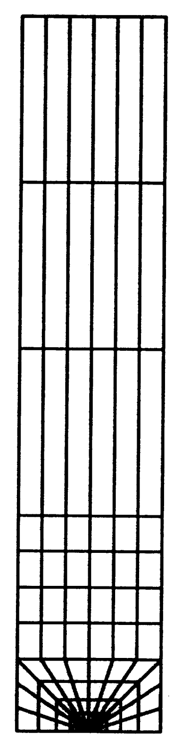

Fig. 3. Finite element mesh of DENT specimen (1/4 model).

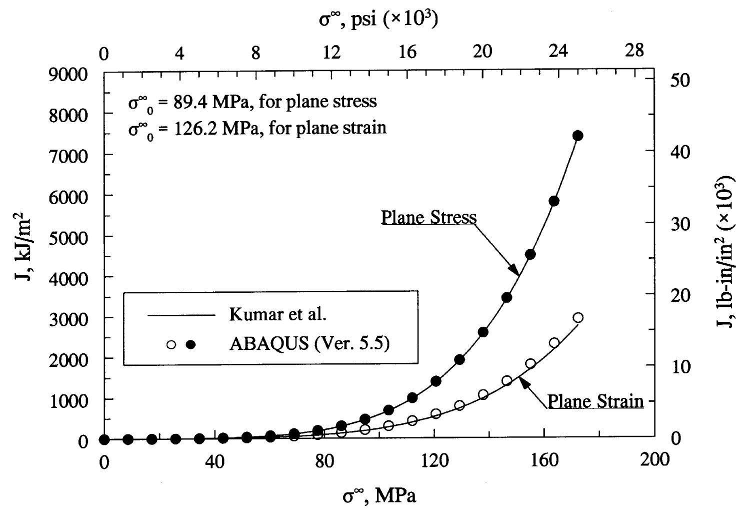

Fig. 4. Comparisons of predicted J for DENT specimen with existing solutions.

probability based on the instability of crack growth is more complicated and is beyond the current capability. In addition, the random crack size can only be modeled for two-dimensional problems. Work is currently ongoing to incorporate fracture instability in the performance criteria and extend the statistical models to include random crack geometry for three-dimensional structures.

6. Numerical examples

6.1. Example 1: A double-edged-notched tension specimen

Consider a two-dimensional double-edged-notched tension (DENT) specimen subjected to quasi-static far-field tension stress σ^∞. The geometry of the DENT specimen, shown in Fig. 2, has width $2W = 1.016$ m (40 in.), length $2L = 5.08$ m (200 in.), and crack length $a =$ 0.254 m (10 in.). The specimen material is TP304 stainless steel and the operating temperature is 288°C (550 F). Both load and material properties were assumed to be random. Table 1 shows the means, coefficients of variation (COV), and probability distributions of these random parameters, obtained from recently performed statistical characterization of actual material property data [5]. The random variables were also assumed to be statistically independent. The deterministic material parameters involved are reference stress $\sigma_0 = 154.78$ MPa (22,450 psi) and Poisson's ratio, $\nu = 0.3$. Note that the Ramberg–Osgood equation (Eq. (1)) has only two independent parameters. In this study, α and n were assumed to vary randomly, while σ_0 was held deterministic [5].

Due to symmetry, a finite element mesh was constructed for only 1/4 model, as shown in Fig. 3. A total of 114 elements and 393 nodes were used in the mesh. Second-order elements from the ABAQUS element library were

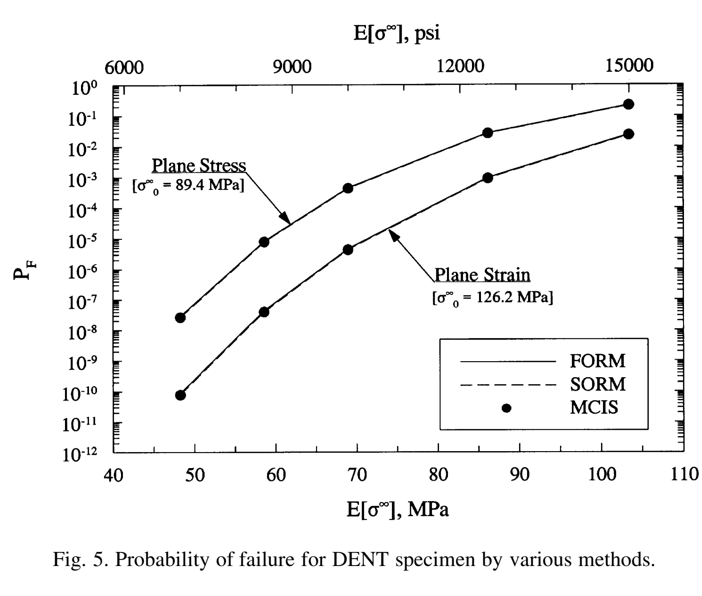

Fig. 5. Probability of failure for DENT specimen by various methods.

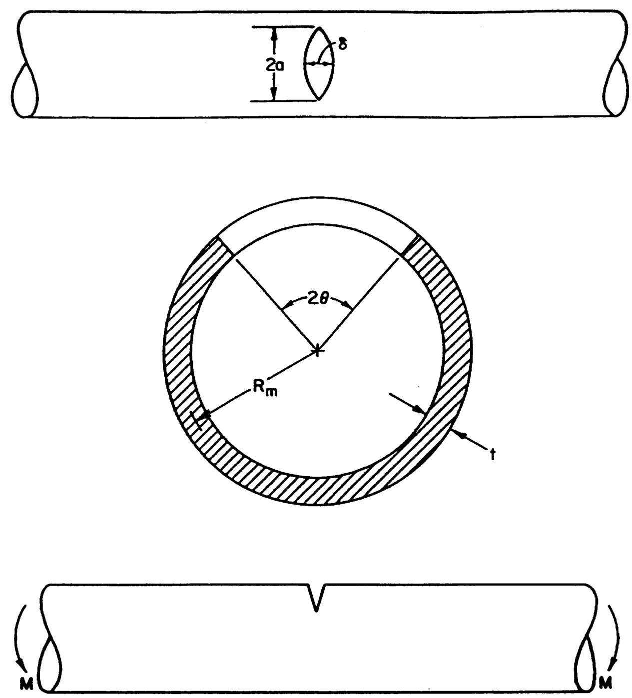

Fig. 6. A TWC pipe subjected to pure bending moment.

used. Both plane stress and plane strain conditions were studied. The reduced integration, eight-noded quadrilaterial element type CPS8R was employed for plane stress. For plane strain, the element type CPE8RH was employed, a mixed formulation element typically used to address the incompressibility constraint for plane strain. Focused elements were used in the vicinity of the crack tip. The material model employed was the deformation theory, Ramberg–Osgood model defined in Eq. (1).

Fig. 4 shows the deterministic results of J from PROFRAC (ABAQUS) as a function of σ^∞ for plane stress and plane strain conditions. The mean values of the material properties, defined in Table 1, were used to generate the plots in Fig. 4. Fig. 4 also presents the corresponding solutions obtained using the method of Kumar et al. [25]. The predicted finite element results from this study match very well with the J-integral solutions of Kumar et al. for the load intensities and material constants considered. The crack driving force (J) is higher for plane stress that for plane strain as expected. Similar results were also obtained by Kumar et al. [25].

Following deterministic validation of J, several probabilistic analyses were performed using PROFRAC to calculate failure probability as a function of mean far-field tensile stress. Fig. 5 shows the results in the form of P_F vs $E[\sigma^\infty]$ plots for both plane stress and plane strain conditions. The failure probabilities increase with the intensity of the mean stress, as expected. Due to the higher demand of J (see Fig. 4), the failure probability in plane stress is generally larger than in plane strain, regardless of the load intensity. The fracture toughness was assumed to be the same for both the plane stress and plane strain conditions in these calculations. Typically, however, the toughness for plane stress is higher than for plane strain. Due to a lack of data, this issue was not investigated in this study.

Fig. 5 presents the results of several reliability methods, including FORM, SORM, and MCIS, used to obtain these probabilities. There are no meaningful differences in the solutions from these three methods. In addition, the results show that accurate estimates of failure probability can be obtained using FORM and SORM, as compared with the results obtained using MCIS.

6.2. Example 2: A through-wall-cracked cylinder specimen

Consider a three-dimensional circumferential through-wall-cracked (TWC) pipe subjected to a remote bending moment M. The pipe has mean radius $R_m = 355.6$ mm (14 in.), wall thickness $t = 25.4$ mm (1 in.), and normalized crack angle $\theta/\pi = 0.125$. The pipe is composed of TP304 stainless steel with an operating temperature of 288°C (550 F). The pipe geometry is shown in Fig. 6.

Table 2 lists the means, COV, and probability distributions of tensile parameters (E, α, n), fracture toughness parameter (J_{Ic}), and bending moment (M). As mentioned previously, the statistics of the material properties were obtained from actual TP304 stainless steel data at 288°C (550 F) [5]. However, the probabilistic characteristics of M were chosen arbitrarily. For this example, $\sigma_0 =$ 154.78 MPa (22,450 psi) and $\nu = 0.3$.

A finite element mesh for the TWC pipe specimen is

Table 2
Statistical properties of random input for TWC pipe specimen

Random variable	Mean	COV[a]	Probability distribution	References
Elastic modulus (E)	182.7 GPa	0.05	Gaussian	–[b]
Ramberg–Osgood coefficient (α)	8.073	0.439	Lognormal	[5]
Ramberg–Osgood exponent (n)	3.8	0.146	Lognormal	[5]
Initiation fracture toughness (J_{Ic})	1242.6 kJ/m^2	0.47	Lognormal	[5]
Bending moment (M)	Variable[c]	0.1	Gaussian	–[b]

[a] COV = standard deviation/mean.
[b] Arbitrarily assumed.
[c] Varies from 1130 to 2260 kN m (10×10^6–20×10^6 lb in.).

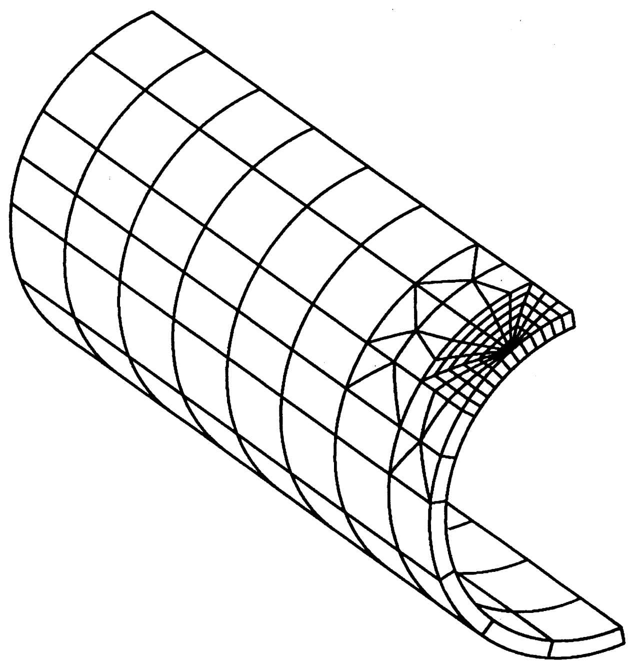

Fig. 7. Finite element mesh of TWC pipe specimen (1/4 model).

shown in Fig. 7. A quarter model was used to take advantage of the symmetry. Twenty-noded isoparametric solid elements (C3D20R) from the ABAQUS library were used, with focused elements at the crack tip. A total of 150 elements and 1098 nodes were used. The stress–strain curve was modeled using the Ramberg–Osgood equation (Eq. (1)) in this example as well.

Fig. 8 shows the deterministic comparisons of the predicted J with the results of the GE/EPRI method [26] using the mean values of random input for the TWC pipe. The continuous lines in Fig. 8 represent the values of J obtained from the GE/EPRI equations using the influence functions derived by Rahman [6], Kumar et al. [26], and Brust et al. [1]. The solid points in Fig. 8 indicate the J solutions from this study involving ABAQUS elastic–plastic analysis. The calculated values of J compare very well with existing solutions found in the literature. The J values from this study are comparatively closer to the Rahman [6] and Brust et al. [1] solutions, which were also based on three-dimensional solid elements as opposed to the shell elements used by Kumar et al. [26].

Fig. 9 plots P_F vs $E[M]$, as obtained using FORM, SORM, and MCIS. No significant differences are found in the probability estimates from these methods. Comparison of the MCIS results with the FORM or SORM results indicates that accurate failure probability estimates can be obtained using the latter two methods. All probabilistic analyses were performed using PROFRAC.

The numerical results presented in this paper are derived solely on EPFM-based failure criterion (i.e. initiation of crack-growth). The likelihood of plastic collapse is not addressed in the present analysis. The calculation of the probability of plastic collapse is much simpler than the analysis presented in this paper and is thoroughly described in the current literature [3,5–9].

7. Summary and conclusions

A probabilistic methodology has been developed for elastic–plastic fracture-mechanics analysis of general cracked structures. The methodology involves nonlinear finite element analysis using the well-established commercial codes; statistical models for uncertainty in material constitutive law, fracture toughness, and loads; and computational reliability methods for evaluating probabilistic characteristics of the J-integral and J-based fracture. The PROFRAC computer code was developed by implementing all the numerical methods presented in this study. Two numerical examples have been presented to illustrate the proposed

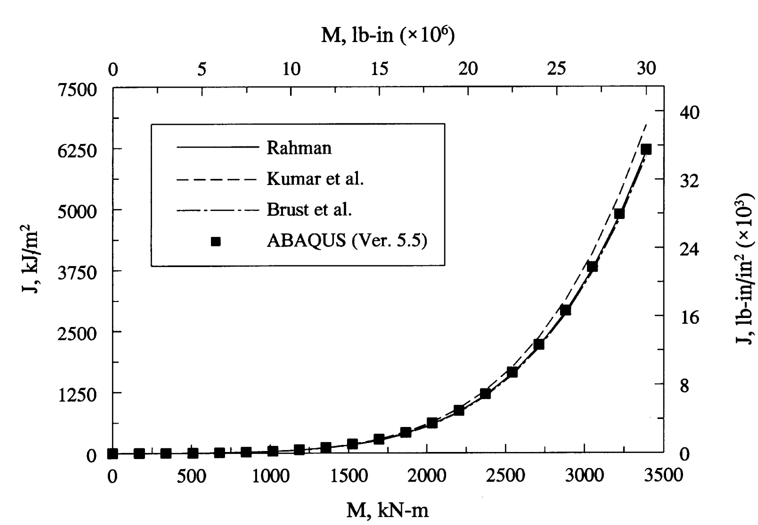

Fig. 8. Comparisons of predicted J for TWC pipe specimen with existing solutions.

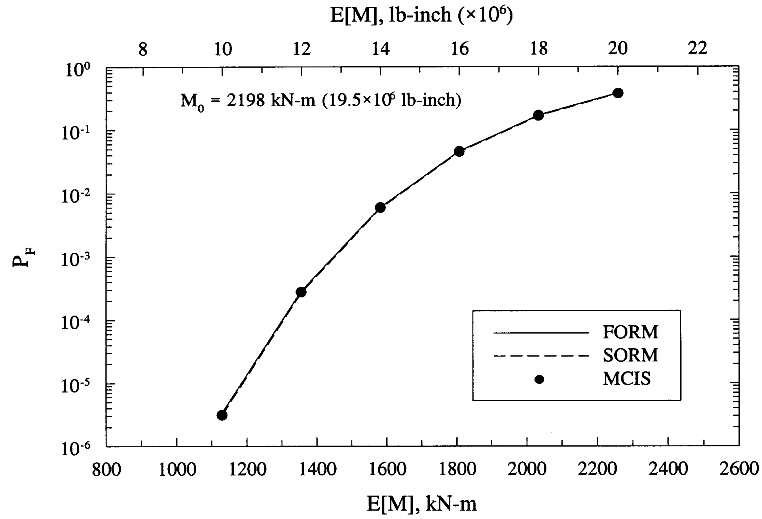

Fig. 9. Probability of failure for TWC pipe specimen by various methods.

methodology for two- and three-dimensional cracked structures. The results from these examples indicate that the methodology is capable of determining accurate deterministic and probabilistic characteristics of the *J*-integral for use in EPFM.

References

[1] Brust FW, Scott P, Rahman S, Ghadiali N, Kilinski T, Francini B, Marschall CW, Miura N, Krishnaswamy P. Assessment of short through-wall circumferential crack in pipes — Experiments and analysis. NUREG/CR-6235, U.S. Nuclear Regulatory Commission, Washington, D.C., April 1995.

[2] Rahman S, Brust F, Ghadiali N, Choi YH, Krishnaswamy P, Moberg F, Brickstad B, Wilkowski G. Refinement and evaluation of crack-opening-area analyses for circumferential through-wall cracks in pipes. NUREG/CR-6300, U.S. Nuclear Regulatory Commission, Washington, D.C., 1995.

[3] Provan, JW. Probabilistic fracture mechanics and reliability. Dordrecht, The Netherlands: Martinus Nijhoff Publishers, 1987.

[4] Wilkowski GM, and others. Short cracks in piping and piping welds Program. NUREG/CR-4599, vols. 1 to 3, nos. 1 and 2. U.S. Nuclear Regulatory Commission, Washington, D.C., 1991–1994.

[5] Rahman S, Ghadiali N, Paul D, Wilkowski G. Probabilistic pipe fracture evaluations for leak-rate-detection applications. NUREG/CR-6004, U.S. Nuclear Regulatory Commission, Washington, D.C., 1995.

[6] Rahman S. A stochastic model for elastic–plastic fracture analysis of circumferential through-wall-cracked pipes subject to bending. Engng Fract Mech 1995;52(2):265–88.

[7] Wilson R, Mitchell BJ, Ainsworth RA. Relationship between conditional failure probabilities and corresponding reserve factors derived from the R6 failure assessment diagram. In: Proceedings of the ASME Pressure Vessel and Piping Conference, Montreal, Canada, July 1996.

[8] Heinfling G, Pendola M, Hornet P. Reliability level provided by safety factor in defect assessment procedures. In: Proceedings of the ASME Pressure Vessel and Piping Conference, Boston, MA, August 1999.

[9] Dillstrom P. ProSINTAP — A probabilistic program implementing the SINTAP assessment procedure. Engng Fract Mech 2000;67:647–68.

[10] Rahman S. Probabilistic fracture mechanics: *J*-estimation and finite element methods. Engng Fract Mech 2001;68:107–25.

[11] Rice JR. A path independent integral and the approximate analysis of strain concentration by notches and cracks. J Appl Mech 1968;35:379–86.

[12] Hutchinson JW. Fundamentals of the phenomenological theory of nonlinear fracture mechanics. J Appl Mech 1983;50:1042–51.

[13] Rice JR, Rosengren GF. Plane strain deformations near a crack tip in a power-law hardening material. J Mech Phys Solids 1968;16:1–12.

[14] Wilkowski GM, and others. Degraded Piping Program — Phase II, Final and Semiannual Reports. NUREG/CR-4082, Vols. 1 to 8. U.S. Nuclear Regulatory Commission, Washington, D.C., 1985–1989.

[15] Schmidt RA, Wilkowski GW, Mayfield M. The international piping integrity research group (IPIRG) program — An overview. In: Proceedings of 11th International Conference on Structural Mechanics in Reactor Technology, Paper G23/1, Tokyo, Japan, August 1991.

[16] Hopper A, Mayfield M, Olson R, Scott P, Wilkowski G. Overview of the IPIRG-2 Program — seismic loaded cracked pipe system experiments. In: Proceedings of 13th International Conference on Structural Mechanics in Reactor Technology, Division F, Paper F12-1, August 1995.

[17] Rahman S, Wilkowski G, Brust F. Fracture analysis of full-scale pipe experiments on stainless steel flux welds. Nucl Engng Des 1996;160:77–96.

[18] Shih CF, Moran B, Nakamura T. Energy release rate along a three-dimensional crack front in a thermally stressed body. Int J Fract 1986;30:79–102.

[19] Moran B, Shih CF. A general treatment of crack tip contour integrals. Int J Fract 1987;35:295–310.

[20] Anderson TL. Fracture mechanics: Fundamentals and applications. 2nd ed. Boca Raton, Florida: CRC Press, 1995.

[21] Madsen HO, Krenk NC, Lind NC. Methods of structural safety. Englewood Cliffs, NJ: Prentice-Hall, 1986.

[22] Hohenbichler M. Improvement of second-order reliability estimates by importance sampling. J Engng Mech ASCE 1988;114(12):2195–9.

[23] ABAQUS, User's Guide and Theoretical Manual, Version 5.5, Hibbitt, Karlsson, and Sorenson, Pawtucket, RI, 1996.

[24] STRUREL — A Structural Reliability Analysis Program, User's and Theoretical Manual, RCP GmbH, Munich, Germany, 1991.

[25] Kumar V, German MD, Shih CF. An engineering approach for elastic–plastic fracture analysis. Palo Alto, CA: Electric Power Research Institute, 1981 (EPRI NP-1931).

[26] Kumar V, German MD, Wilkening WW, Andrews WR, deLorenzi HG, Mowbray DF. Advances in elastic–plastic fracture analysis. Palo Alto, CA: Electric Power Research Institute, 1984 (EPRI NP-3607).